https://dx.doi.org/10.4314/wojast.v16i2.233

ISSN: 2141 – 3290
www.wojast.com

NUMERICAL SOLUTION OF SCHRÖDINGER EQUATION WITH SCREENED KRATZER ECKART POTENTIAL VIA FINITE DIFFERENCE METHOD

***ANTIA, A. D. AND OKON, U. A.**
Theoretical Physics Group, Department of Physics,
University of Uyo, Nigeria
****CORRESPONDENCE**: akaninyeneantia@uniuyo.edu.ng*

ABSTRACT

The numerical solution to the time-independent Schrödinger equation (TISE) for hydrogen-related diatomic molecules was obtained using the finite difference method (FDM) for the Screened-Kratzer-Eckart Potential (SKEP) system. With the SKEP, the study explores the quantum behaviour of molecular systems by discretising the TISE and solving the resulting eigenvalue problem. MATLAB was employed to implement the numerical scheme, generating the energy eigenvalues and corresponding eigenfunctions. The results obtained demonstrate consistency with theoretical expectations and existing analytical models, validating the effectiveness of the finite difference approach. This study contributes to the understanding of molecular quantum systems and offers a computational framework applicable to a wide range of quantum mechanical problems involving complex potentials.

KEYWORDS: Screened-Kratzer-Eckart Potential, Schrödinger equation, Numerical solutions, Finite Difference Method

INTRODUCTION

The Schrödinger equation is a fundamental equation in quantum mechanics, describing the wave-like behavior of particles in quantum systems and providing the basis for understanding their energy levels and wave functions. It is pivotal in fields such as quantum chemistry and molecular physics, where it enables the analysis of atomic and molecular structures, including diatomic molecules. Analytical solutions to the Schrödinger equation are available for simple systems like the hydrogen atom or harmonic oscillator (Griffiths, 2005). However, for complex systems with realistic interaction potentials, such as diatomic molecules, analytical solutions are often unattainable, necessitating numerical methods. One such complex potential is the Screened-Kratzer-Eckart Potential (SKEP), a model used to describe the interaction between atoms in diatomic molecules under screened conditions, such as in vacuum or superconducting states. The SKEP combines features of the Kratzer potential, which includes Coulombic and centrifugal-like terms, and the Eckart potential, which introduces exponential screening to account for short-range interactions. The specific form of the SKEP addressed in this paper is given as:

$$V(r) = V_0\left(1 - \frac{ge^{-\alpha r}}{1-e^{-\alpha r}}\right)^2 - \mathrm{V}_1\left(\frac{A}{r} - \frac{B}{2r^2}\right)e^{-\alpha r} \qquad (1)$$

where: $g = e^{\alpha r_e} - 1,\ A = r_e, B = r_e^2, V_0 = D_e, \mathrm{V}_1 = 2D_e$

D_e is the dissociation energy, r_e is the equilibrium bond length, r is the inter-atomic distance and α is the screening parameter.

This potential combine screened exponential terms with inverse radial dependencies, making it suitable for modeling the Ro-vibrational energy levels of diatomic molecules under conditions where screening effects are significant, such as in condensed matter or high-pressure environments. Exponential-like potentials have significant applications in physics are well studied (Antia *et al.*, 2022 and Isonguyo *et al.,* 2022).

The Finite Difference Method (FDM) is a widely used numerical technique for approximating solutions to differential equations, particularly in problems involving boundary conditions (Sullivan, 2005 and Sullivan and Citrin, 2002). It works by discretizing the continuous domain into a grid and replacing derivatives with finite difference expressions, which leads to a system of algebraic equations that can be solved computationally. In the context of quantum mechanics, this approach is particularly effective for the time-independent Schrödinger equation, where it enables the calculation of energy eigenvalues and corresponding wavefunctions for systems with complex potentials (Griffiths, 2005 and Press *et al.,* 2007).

In this study, the FDM is applied to solve the radial Schrödinger equation involving the Screened-Kratzer-Eckart Potential (SKEP) a potential that combines exponential and inverse power-law terms and does not permit exact analytical solutions. The method discretizes the radial coordinate and approximates the second derivative using central differences, leading to a tridiagonal Hamiltonian matrix whose eigenvalues correspond to the quantized energy levels of the system (Dong *et al.,* 2016).

The choice of FDM over other methods, such as the finite element method or variational techniques, is based on several compelling advantages. Firstly, FDM is simple to implement and conceptually intuitive, especially for one-dimensional or radial problems. Secondly, it provides high accuracy with manageable computational cost, making it suitable for modeling molecular systems with non-trivial potentials like the SKEP. Thirdly, it integrates efficiently with platforms such as MATLAB, which offers robust matrix operations and visualization tools (Vandrevala, 2014). Moreover, FDM handles boundary conditions naturally and

https://dx.doi.org/10.4314/wojast.v16i2.233

does not require prior knowledge of the form of the wavefunction, making it flexible for a wide range of physical systems (Ismail and Osman, 2019). Given these strengths, the FDM was chosen as a reliable and efficient numerical approach to explore the ro-vibrational energy spectra of diatomic molecules under the influence of the SKEP in this paper.

The Radial Schrödinger Equation

The time-independent Schrödinger equation (Griffiths, 2005) is given as:

$$-\frac{\hbar^2}{2m}\nabla^2\psi(r) + V(r)\psi(r) = \mathrm{E}\psi(r), \tag{2}$$

where $\hbar$ is the reduced Planck's constant, m is the mass of the particle, ∇^2 is the Laplacian operator, $V(r)$ is the potential energy, E is the total energy, and $\psi(r)$ is the wave function. For systems with central potentials, it is convenient to express the Schrödinger equation in spherical coordinates, where the Laplacian operator takes the form:

$$\nabla^2 = \frac{\partial}{\partial r}(r^2\frac{\partial}{\partial r}) + \frac{1}{r^2\sin\theta}\frac{\partial}{\partial\theta}(\sin\theta\frac{\partial}{\partial\theta}) + \frac{1}{r^2\sin^2\theta}\frac{\partial^2}{\partial\phi^2} \tag{3}$$

We assume the wave function can be separated as:

$$\psi(r,\theta,\phi) = R(r)Y_l^m(\theta,\phi) \tag{4}$$

$R(r)$ is the radial wave function Y_l^m are the spherical harmonics, which satisfy the eigenvalue equation for the angular momentum operator:

$$\hat{L}^2Y_l^m(\theta,\phi) = l(l+1)\hbar^2Y_l^m(\theta,\phi) \tag{5}$$

After separating variables, the radial Schrödinger equation takes the form:

$$-\frac{\hbar^2}{2m}\left[\frac{1}{r^2}\frac{d}{dr}\left(r^2\frac{dR}{dr}\right)\right] + \left[V(r) + \frac{l(l+1)\hbar^2}{2mr^2}\right]R(r) = ER(r) \tag{6}$$

Rewriting,

$$\frac{d^2R}{dr^2} + \frac{2}{r}\frac{dR}{dr} + \left[\frac{2m}{\hbar^2}(E - V(r)) - \frac{l(l+1)}{r^2}\right]R(r) = 0 \tag{7}$$

where,

$$V_{\text{eff}}(r) = V(r) + \frac{l(l+1)\hbar^2}{2mr^2} \tag{8}$$

is the effective potential, incorporating both the actual potential and the centrifugal barrier.

where $V(r)$ is the Screened-Kratzer-Eckart potential given in equation (1)

To simplify, we define a new function:

$$R(r) = \frac{u(r)}{r} \tag{9}$$

which transforms the equation into:

$$\frac{d^2u}{dr^2} + \left[\frac{2m}{\hbar^2}(E - V_{\text{eff}}(r))\right]u(r) = 0 \tag{10}$$

This is a simplified Schrödinger equation for,$u(r)$ which is more suitable for numerical solutions.

Finite Difference Method for Solving the Schrödinger Equation

Since analytical solutions to the Schrödinger equation are not always possible, numerical techniques such as the finite difference method (FDM) provide an alternative approach. This method discretizes the second-order differential equation into a system of linear equations that can be solved using matrix techniques. We can find an approximate solution to the Schrodinger equation by transforming the differential equation into a matrix equation. If we divide the x-axis up into a grid of n equally spaced points $(x_1, x_2, \ldots x_n)$ we can express the wavefunction as:

$$|\psi\rangle = \begin{bmatrix}\psi(x_1)\\ \psi(x_2)\\ \vdots\\ \psi(x_n)\end{bmatrix}, \tag{11}$$

where each $\psi(x_i)$ gives the value of the wavefunction at the point x_i. We then express the Hamiltonian as a matrix operator (Vandrevala, 2014).

Discretization of the Schrödinger Equation

Using the finite difference method, the second derivative in the radial Schrödinger equation:

$$\frac{d^2u}{dr^2} = -\left[\frac{2m}{\hbar^2}(E - V_{\text{eff}}(r))\right]u(r) \tag{12}$$

is approximated by a central difference formula:

$$\frac{d^2u}{dr^2} \approx \frac{u_{i+1} - 2u_i + u_{i-1}}{\Delta r^2} \tag{13}$$

where u_i represents the wave function at discrete radial points r_i and Δr is the step size in the radial direction.

Substituting this into the Schrödinger equation, we obtain:

$$\frac{u_{i+1} - 2u_i + u_{i-1}}{\Delta r^2} + \left[\frac{2m}{\hbar^2}(E - V_{\text{eff}}(r_i))\right]u_i = 0 \tag{14}$$

which can be rewritten as:

$$-u_{i+1} + (2 + \Delta r^2K_i)u_i - u_{i-1} = 0 \tag{15}$$

Where:

$$K_i = \frac{2m}{\hbar^2}(E - V_{\text{eff}}(r_i)) \tag{16}$$

Construction of the Hamiltonian Matrix

Rearranging the finite difference equation, we can express it in matrix form:

$$Hu = Eu \tag{17}$$

where H is the Hamiltonian matrix given by:

https://dx.doi.org/10.4314/wojast.v16i2.233

$$H = \begin{bmatrix} 2+\Delta r^2 K_1 & -1 & 0 & 0 & \dots & 0 \\ -1 & 2+\Delta r^2 K_2 & -1 & 0 & \dots & 0 \\ 0 & -1 & 2+\Delta r^2 K_3 & -1 & \dots & 0 \\ \vdots & \vdots & \vdots & \vdots & \ddots & -1 \\ 0 & 0 & 0 & -1 & 2+\Delta r^2 K_{N-1} & -1 \\ 0 & 0 & 0 & 0 & -1 & 2+\Delta r^2 K_N \end{bmatrix} \quad (18)$$

Solving the eigenvalue problem for $\boldsymbol{H}$ gives the energy eigenvalues $\boldsymbol{E}$ and eigenfunctions $\boldsymbol{u}(\boldsymbol{r})$.

RESULTS AND DISCUSSION

This section presents the numerical results obtained from solving the radial Schrödinger equation for diatomic molecules under the Screened-Kratzer-Eckart potential (SKEP) using the finite difference method (FDM). The computations were performed using MATLAB, the eigenvalue problem given in equation (18) was used to for the computation. The study systematically explores the influence of the principal quantum number (n), the angular momentum quantum number (l), and the screening parameter (α) on the energy spectrum, with n ranging from 1 to 5, (l) from 0 to 3, and (α) from 0.1 to 0.3. These parameters were selected to capture a broad range of quantum states and screening effects, providing insights into the behaviour of molecular systems under varying conditions. The results are presented through detailed tables and graphical representations, highlighting key trends and their implications for quantum mechanics and molecular physics. By comparing these findings with existing literature (Udoh *et al.,* 2024), this section validates the numerical approach and underscores its relevance to real-world applications, such as spectroscopic analysis and material characterisation in screened environments. The spectroscopic parameters in Table 1 were used in the computation with $\hbar$=1.0.

Table 1: Spectroscopic parameters for the selected diatomic molecules (Qiang and Dong, 2010)

Molecules	$\boldsymbol{D_e}$(eV)	$\boldsymbol{r_e}$(Å)	α(Å^{-1})	m(a.m.u)
H_2	4.7446	0.7416	1.9426	0.050391
HCl	4.6190	1.2746	1.8677	0.980105
LiH	2.5152	1.5956	1.1280	0.880122

Table 2: Ro-vibrational energy eigenvalue of the SKEP for H_2 molecules at α = 0.1

n	l	E_{nl}, α= 0.1	l	E_{nl}, α=0.1	l	E_{nl}, α=0.1	l	E_{nl}, α=0.1
1	0	-4.38895	1	-4.38888	2	-4.38873	3	-4.38851
2	0	-4.35066	1	-4.35059	2	-4.35045	3	-4.35023
3	0	-4.31259	1	-4.31252	2	-4.31238	3	-4.31216
4	0	-4.27474	1	-4.27467	2	-4.27453	3	-4.27431
5	0	-4.23710	1	-4.23703	2	-4.23689	3	-4.23668

Table 3: Ro-vibrational energy eigenvalue of the SKEP for H_2 molecules at α = 0.2

n	l	E_{nl}, α= 0.2	l	E_{nl}, α=0.2	l	E_{nl}, α=0.2	l	E_{nl}, α=0.2
1	0	-4.07959	1	-4.07951	2	-4.07936	3	-4.07914
2	0	-4.03965	1	-4.03957	2	-4.03942	3	-4.03920
3	0	-3.99993	1	-3.99986	2	-3.99971	3	-3.99949
4	0	-3.96044	1	-3.96037	2	-3.96022	3	-3.96000
5	0	-3.92117	1	-3.92110	2	-3.92095	3	-3.92074

Table 4: Ro-vibrational energy eigenvalue of the SKEP for H_2 molecules at α = 0.3

n	l	E_{nl}, α= 0.3	l	E_{nl}, α=0.3	l	E_{nl}, α=0.3	l	E_{nl}, α=0.3
1	0	-3.79447	1	-3.79439	2	-3.79424	3	-3.79401
2	0	-3.75307	1	-3.75299	2	-3.75284	3	-3.75261
3	0	-3.71190	1	-3.71182	2	-3.71167	3	-3.71145
4	0	-3.67097	1	-3.67089	2	-3.67074	3	-3.67052
5	0	-3.63026	1	-3.63019	2	-3.63004	3	-3.62981

Table 5: Ro-vibrational energy eigenvalue of the SKEP for HCl molecules at α = 0.1

n	l	E_{nl}, α= 0.1	l	E_{nl}, α=0.1	l	E_{nl}, α=0.1	l	E_{nl}, α=0.1
1	0	-4.54256	1	-4.54236	2	-4.54196	3	-4.54136
2	0	-4.48201	1	-4.48181	2	-4.48141	3	-4.48082
3	0	-4.42208	1	-4.42188	2	-4.42149	3	-4.42090
4	0	-4.36277	1	-4.36257	2	-4.36218	3	-4.36160
5	0	-4.30406	1	-4.30387	2	-4.30348	3	-4.30291

https://dx.doi.org/10.4314/wojast.v16i2.233

Table 6: Ro-vibrational energy eigenvalue of the SKEP for HCl molecules at α = 0.2

n	l	E_{nl}, α= 0.2	l	E_{nl}, α=0.2	l	E_{nl}, α=0.2	l	E_{nl}, α=0.2
1	0	-4.49701	1	-4.49680	2	-4.49640	3	-4.49580
2	0	-4.43601	1	-4.43581	2	-4.43541	3	-4.43482
3	0	-4.37564	1	-4.37545	2	-4.37505	3	-4.37446
4	0	-4.31590	1	-4.31570	2	-4.31531	3	-4.31473
5	0	-4.25676	1	-4.25657	2	-4.25619	3	-4.25561

Table 7: Ro-vibrational energy eigenvalue of the SKEP for HCl molecules at α = 0.3

n	l	E_{nl}, α= 0.3	l	E_{nl}, α=0.3	l	E_{nl}, α=0.3	l	E_{nl}, α=0.3
1	0	-4.45210	1	-4.45180	2	-4.45139	3	-4.45079
2	0	-4.39057	1	-4.39037	2	-4.38998	3	-4.38938
3	0	-4.32978	1	-4.32959	2	-4.32919	3	-4.32860
4	0	-4.26961	1	-4.26942	2	-4.26903	3	-4.26844
5	0	-4.21006	1	-4.20987	2	-4.20948	3	-4.20890

Table 8: Ro-vibrational energy eigenvalue of the SKEP for LiH molecules at α = 0.1

n	l	E_{nl}, α= 0.1	l	E_{nl}, α=0.1	l	E_{nl}, α=0.1	l	E_{nl}, α=0.1
1	0	-2.46644	1	-2.46622	2	-2.46578	3	-2.46511
2	0	-2.41948	1	-2.41926	2	-2.41882	3	-2.41816
3	0	-2.37318	1	-2.37297	2	-2.37253	3	-2.37187
4	0	-2.32754	1	-2.32733	2	-2.32691	3	-2.32627
5	0	-2.28255	1	-2.28240	2	-2.28192	3	-2.28129

Table 9: Ro-vibrational energy eigenvalue of the SKEP for LiH molecules at α = 0.2

n	l	E_{nl}, α= 0.2	l	E_{nl}, α=0.2	l	E_{nl}, α=0.2	l	E_{nl}, α=0.2
1	0	-2.44158	1	-2.44136	2	-2.44091	3	-2.44024
2	0	-2.39427	1	-2.39405	2	-2.39362	3	-2.39296
3	0	-2.34764	1	-2.34743	2	-2.347699	3	-2.34634
4	0	-2.30167	1	-2.30146	2	-2.30103	3	-2.30039
5	0	-2.25635	1	-2.25614	2	-2.25572	3	-2.25508

Table 10: Ro-vibrational energy eigenvalue of the SKEP for LiH molecules at α = 0.3

n	l	E_{nl}, α= 0.3	l	E_{nl}, α=0.3	l	E_{nl}, α=0.3	l	E_{nl}, α=0.3
1	0	-2.41702	1	-2.41680	2	-2.41635	3	-2.41568
2	0	-2.36938	1	-2.36916	2	-2.36872	3	-2.36806
3	0	-2.32242	1	-2.32220	2	-2.32177	3	-2.32111
4	0	-2.27612	1	-2.27591	2	-2.27548	3	-2.27483
5	0	-2.23048	1	-2.23026	2	-2.22984	3	-2.22920

Further analyses of the ro-vibrational energy eigenvalues for the diatomic molecules H_2, HCl, and LiH are presented in Tables 2 through 10 and illustrated in Figures 1 through 5 which reveal the effects of the screening parameter α, principal quantum number n, orbital angular momentum quantum number l, dissociation energy D_e, and equilibrium bond length r_e on the energy spectra. These findings are interpreted in the context of quantum mechanics and compared with existing literature (Udoh *et al.,* 2024) to validate the numerical approach. H_2 Molecule at α = 0.1, 0.2, and 0.3 is presented in Tables 2-4 respectively which indicate the energy eigenvalues for H_2 across different quantum states and screening parameters. In Table 2, for n = 1 and l = 0, the energy is -4.38895 eV, increasing to -4.23710 eV at n = 5, indicating that higher principal quantum numbers correspond to less negative (higher) energy states, as expected for quantized bound systems. As l increases from 0 to 3 at n = 1, the energy shifts slightly from -4.38895 eV to -4.38851 eV, reflecting the influence of the centrifugal barrier. In Table 3, the energy for n = 1, l = 0 is -4.07959 eV, and in Table 4, it is -3.79447 eV. This trend of less negative energies with increasing α suggests that greater screening weakens the potential, reducing the binding energy.

Tables 5-7 represent the HCl molecule at α = 0.1, 0.2, and 0.3 respectively. Table 5 shows the energy at n = 1, l = 0 as -4.54256 eV, rising to -4.30406 eV at n = 5, consistent with the quantization pattern observed in H_2. The slight increase with l, from -4.54256 eV (l = 0) to -4.54136 eV (l = 3) at n = 1, again highlights the centrifugal effect. Table 6 reports -4.49701 eV for n = 1, l = 0, and Table 7 (α = 0.3) shows -4.45210 eV. The less negative energies as α increases

https://dx.doi.org/10.4314/wojast.v16i2.233

indicate a similar screening effect as in H_2, though the absolute values differ due to HCl's distinct spectroscopic parameters (D_e = 4.6190 eV, r_e= 1.2746 Å). The behaviour of LiH molecule for the screening parameter α = 0.1, 0.2 and 0.3 are presented in Tables 8, 9 and 10 respectively. Table 8 (α = 0.1) gives an energy of -2.46644 eV at n = 1, l = 0, increasing to -2.28255 eV at n = 5, following the same trend of higher energy with increasing n. The energy shifts from -2.46644 eV (l = 0) to -2.46511 eV (l = 3) at n = 1. Table 9 (α = 0.2) lists -2.44158 eV, and Table 10 (α = 0.3) lists -2.41702 eV for n = 1, l = 0. The reduction in binding energy with increasing α is evident, though LiH's energies are less negative overall, reflecting its lower dissociation energy (D_e = 2.5152 eV) compared to H_2 and HCl.

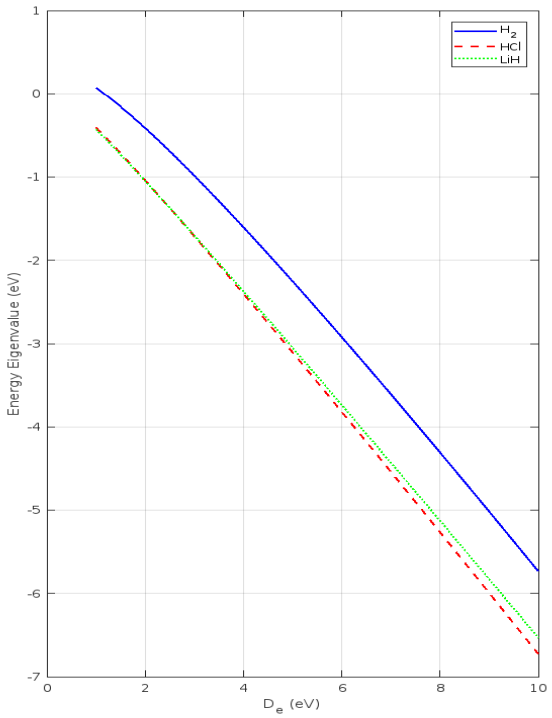

Figure 1: Energy vs dissociation energy (D_e)

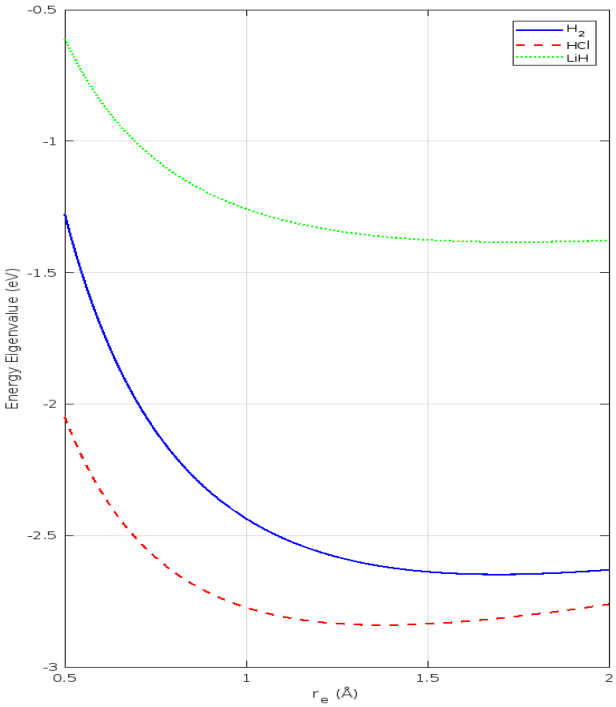

Figure 2: Energy vs equilibrium bond length (r_e)

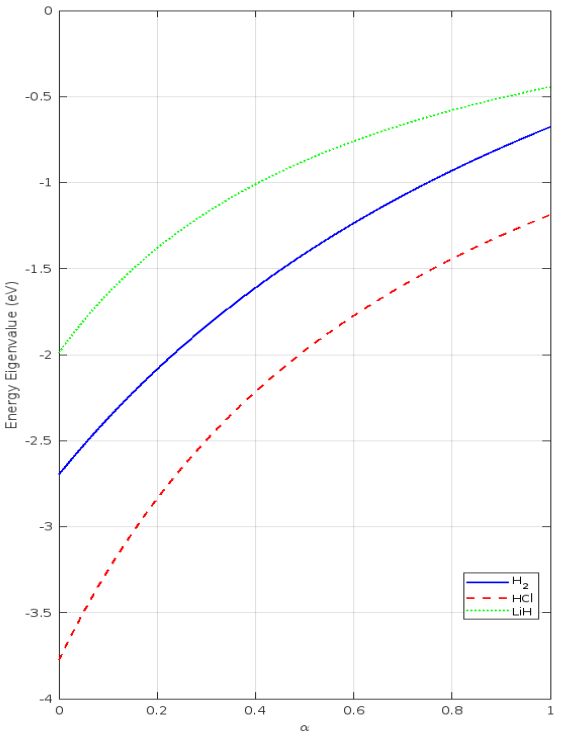

Figure 3: Energy vs screening parameter (α)

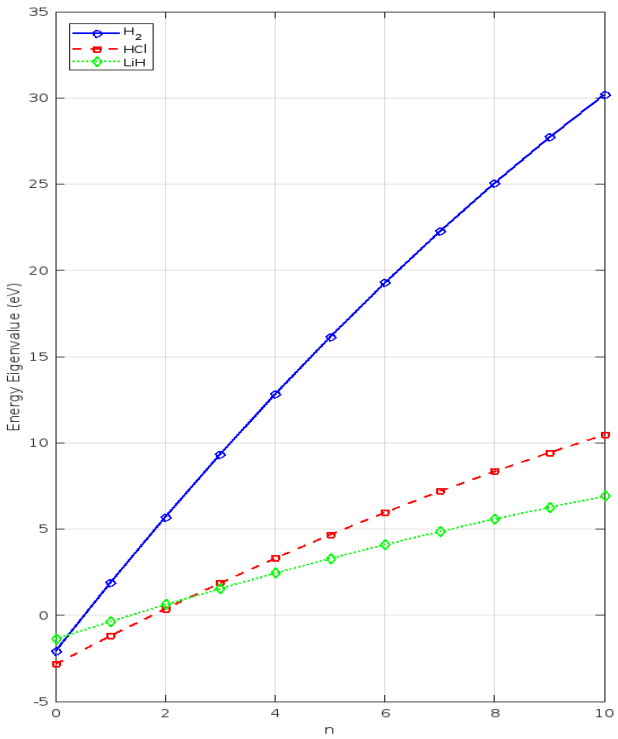

Figure 4: Energy vs principal quantum number (n)

https://dx.doi.org/10.4314/wojast.v16i2.233

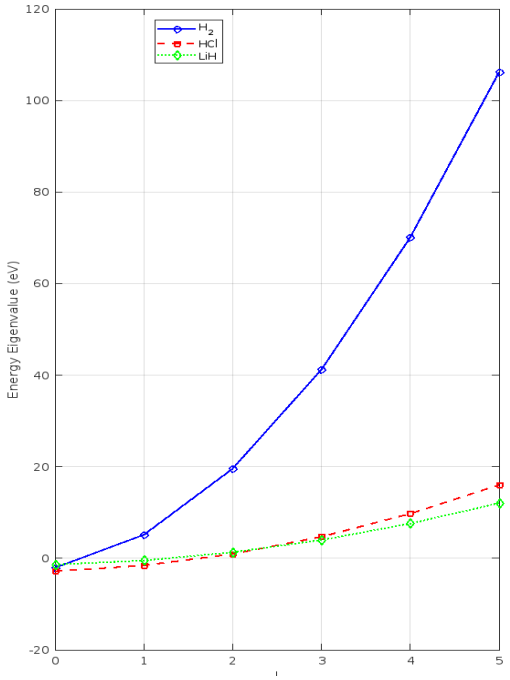

Figure 5: Energy vs orbital angular momentum quantum number (l)

Figure 1 gives the variation of energy eigenvalues with the dissociation energy (D_e) a key parameter defining the potential well's depth. Given that D_e values are 4.7446 eV (H_2), 4.6190 eV (HCl), and 2.5152 eV (LiH), the figure likely shows more negative energies for molecules with higher D_e, as a deeper potential well enhances binding. This explains why H_2 and HCl exhibit more negative energies than LiH across all tables. Figure 2 illustrates energy dependence on the equilibrium bond length, r_e (0.7416 Å for H_2, 1.2746 Å for HCl, 1.5956 Å for LiH). The equilibrium bond length affects the potential's minimum position. While the exact trend is not deducible without the figure, a larger r_e may shift the energy levels due to changes in the potential's radial dependence, potentially leading to less negative energies for molecules like LiH with greater r_e. Figure 3 is the variation of energy screening parameter. It confirms the tabular trend: as α increases from 0.1 to 0.3, energies become less negative. For H_2, the shift from -4.38895 eV to -3.79447 eV ($n = 1, l = 0$) across Tables 2-4 would appear as an upward curve, reflecting the screening effect that weakens the attractive potential, a hallmark of the SKEP. While Figure 4 shows energy increasing with the principal quantum number n, as seen in all tables (e.g., -4.38895 eV to -4.23710 eV for H_2 at $\alpha = 0.1, l = 0$). This staircase pattern is characteristic of quantized energy levels, with each step representing a higher vibrational state within the potential well. The behaviour energy with orbital angular momentum quantum number (l) is shown in Figure 5. This depicts a slight energy increase with l, such as from -4.38895 eV ($l = 0$) to -4.38851 eV ($l = 3$) for H_2 at $\alpha = 0.1$, $n = 1$. This subtle rise, driven by the centrifugal barrier, would appear as a gentle upward trend, more pronounced at higher l values. The consistent increase in energy with n across all molecules aligns with quantum mechanical expectations for bound states. The slight rise with l reflects the centrifugal term's contribution to the effective potential. The screening parameter α's effect reducing binding energy as it increases is a physical consequence of the SKEP's exponential screening, validated by similar findings in Udoh *et al.* (2024). The FDM's ability to capture these trends underscores its efficacy for complex potentials, offering a robust alternative to analytical methods.

CONCLUSION

In this work, the finite difference method was successfully applied to numerically solve the time-independent Schrödinger equation for a particle under the influence of the Screened-Kratzer-Eckart potential. The computed energy eigenvalues and eigenfunctions provide insight into the quantum mechanical properties of hydrogen-related diatomic molecules. The results confirm the robustness and accuracy of the finite difference method as a practical tool for solving quantum systems where analytical solutions are difficult or impossible to obtain. This approach not only enhances the computational study of molecular interactions but also serves as a foundation for further research into more complex potentials and higher-dimensional quantum systems.

REFERENCES

Antia, A. D., Okon, I. B., Isonguyo, C. N., Akankpo, A. O. and Eyo, N. E. (2022). Bound state solutions and thermodynamic properties of modified exponential screened plus Yukawa potential, *Journal of the Egyptian Mathematical Society*, 30(1):11 https://doi.org/10.1186/s42787-022-00145-y.

Dong, S., Sun, G. H., Falaye, B. J., and Dong, S. H. (2016). Semi-exact solutions to position-dependent mass Schrödinger problem with a class of hyperbolic potential Votanh(ax). *European Physical Journal Plus*, 131, 176.

Griffiths, D. J. (2005). *Introduction to Quantum Mechanics* (2nd ed.). Pearson Education.

Ismail, M. A., and Osman, K. I. (2019). Numerical treatment of time-independent Schrödinger equation using finite difference method. *Malaysian Journal of Fundamental and Applied Sciences*, 15(3), 362–368.

Isonguyo, C. N., Okon, I. B., Antia, A. D., Oyewumi, K. J., Omugbe, E., Onate, C. A., Joshua, R. U., Udoh, M. E., Ituen, I. E. and Araujo, J. P. (2022). Eigensolutions and Thermodynamic Properties of Kratzer Plus Generalized Morse Potential. *Frontiers in Physics*, Volume 10. Doi:10.3389/fphy.2022.962717.

Messiah, A. (1999). Quantum Mechanics. Dover Publications

Press, W. H., Teukolsky, S. A., Vetterling, W. T., and Flannery, B. P. (2007). *Numerical Recipes: The Art of Scientific Computing* (3rd ed.). Cambridge University Press.

Qiang, W. C. and Dong, S. H. (2010). Proper quantization rule. The European Physics Letters, 89,10003.

Ibrahim, N., Okorie, U. S., Sulaiman, N., Rampho, G. J. and Ramantswana, M. (2022). Solutions of the Schrödinger

https://dx.doi.org/10.4314/wojast.v16i2.233

equation of the shifted screened Kratzer potential model using the extended Nikiforov–Uvarov method. *Frontiers in Physics*, 10, 988279.

Plokhotnikov, K. E. (2021). Solving the Schrödinger equation on the basis of finite-difference and Monte-Carlo approaches. Journal of Applied Mathematics and Physics, 9: 328-369.

Sullivan, D. M. and Citrin, D. S. (2005). Determining quantum eigenfunctions in three-dimensional nanoscale structures. *Journal of Applied Physics*, 9(10): 104305-6

Sullivan, D. M. (2005). Determining a complete three-dimensional set of eigenfunctions for nanoscale structure analysis. *Journal of Applied Physics*, 98(1): 084311

Udoh, M. E., Antia A. D., Ikot, A. N., Okorie, U. S., Isonguyo, C. N., Okon, I. B., and Iquen, E. E. (2024). Eigen Solutions of Schrödinger Equation with Screened-Kratzer-Eckart Potential for Diatomic Molecules. *Researchers Journal of Science and Technology*, 4(2), 48–59.

Vandrevala, C. (2014, November 2). *The finite difference method and Schrödinger's equation*. Cupcake Physics. https://cupcakephysics.com/computational%20physics/2014/11/02/the-finite-difference-method-and-schrodingers-equation.html